Manuscript Number:

Title: Influence of the gas-liquid flow configuration in the absorption column on photosynthetic biogas upgrading in algal-bacterial photobioreactors

Article Type: Original research paper

Keywords: Algal-bacterial photobioreactor; biogas upgrading; bio-methane; nutrients recovery; digestate

Corresponding Author: Mr. Raul Munoz, PhD

Corresponding Author's Institution: Valladolid University

First Author: Alma Toledo-Cervantes, PhD

Order of Authors: Alma Toledo-Cervantes, PhD; Cindy Madrid-Chirinos, BSc; Sara Cantera, MSc; Raquel Lebrero, PhD; Raul Munoz, PhD

Abstract: The potential of an algal-bacterial system consisting of a high rate algal pond (HRAP) interconnected to an absorption column (AC) via recirculation of the cultivation broth for the upgrading of biogas and digestate was investigated. The influence of the gas-liquid flow configuration in the AC on the photosynthetic biogas upgrading process was assessed. AC operation in a co-current configuration enabled to maintain a biomass productivity of 15 g m-2 d-1, while during counter-current operation biomass productivity decreased to 8.7 ± 0.5 g m-2 d-1 as a result of trace metal limitation. A bio-methane composition complying with most international regulatory limits for injection into natural gas grids was obtained regardless of the gas-liquid flow configuration. Furthermore, the influence of the recycling liquid to biogas flowrate (L/G) ratio on bio-methane quality was assessed under both operational configurations obtaining the best composition at an L/G ratio of 0.5 and co-current flow operation.

Suggested Reviewers: Leslie Meier PhD
Universidad de La Frontera, Chile
l.meier01@ufromail.cl
Expert in wastewater treatment and Biogas upgrading using microalgae cultures

Cheng Yan Chen PhD
School of Environmental Studies, China
yancheng622@126.com
Expert in digestate treatment and Biogas upgrading using microalgae cultures

Simon Murray PhD
Queen's University Belfast, UK
s.murray@qub.ac.uk
Expert in Biogas upgrading

Enrica Uggetti PhD
Universitat Politècnica de Catalunya, Spain
enrica.uggetti@upc.edu
Expert in wastewater and sludge treatment, low cost technologies,
microalgae, anaerobic digestion and biogas.

Environmental *Group*
Technology
University of Valladolid

Ashok Pandey
Centre of Innovative and
applied Bioprocessing (CIAB)
Mohali, Punjab, India

Dear Editor-in-Chief

Please find enclosed our original unpublished paper "**Influence of the gas-liquid flow configuration in the absorption column on photosynthetic biogas upgrading in algal-bacterial photobioreactors**" co-authored by Alma Toledo-Cervantes, Cindy Madrid-Chirinos, Sara Cantera, Raquel Lebrero and Raúl Muñoz. All authors are aware of the ethics policy of *Bioresource Technology* Journal, declare no conflict of interest and accept responsibility for the present manuscript. The manuscript is submitted for publication in *Bioresource Technology* for the first time, considering that it is the best-suited journal for the research area of the present work, more specifically *Biological waste treatment: Environmental bioengineering* (20.100).

Photosynthetic biogas upgrading coupled with nutrient removal from digestate represents a competitive and environmentally friendly technology to conventional physical-chemical technologies for biogas upgrading. This innovative technology, here evaluated at pilot scale, consisted of a high rate algal pond (HRAP) treating digestate interconnected to a CO_2-H_2S absorption column (AC) via recirculation of the HRAP cultivation broth for biogas scrubbing. Preliminary studies in our lab have consistently showed that despite the high potential of photosynthetic biogas upgrading, N_2 and O_2 stripping from the recycling cultivation broth to the upgraded biogas often results in CH_4 concentrations < 95 % (the minimum concentration for biomethane injection into natural gas grids in most EU countries). Thus, an optimization of biogas scrubbing in the AC of this photosynthetic biogas upgrading system is needed in order to obtain a bio-methane complying with the quality standards for injection into natural gas grids.

This research assessed the influence of the gas/liquid flow configurations (co-current and counter-current) in the AC on bio-methane quality and nutrient recovery from a real digestate in the form of algal-bacterial biomass. The influence of the liquid recycling to biogas flowrate (L/G) ratio on bio-methane quality was also tested under both gas-liquid flow configurations in order to minimize both O_2 and N_2 content in the bio-methane. Additionally, an innovative process design was evaluated by interconnecting an external coagulation-flocculation tank to the HRAP, which allowed obtaining a biomass productivity of 15 g m^{-2} d^{-1} (thus maximizing the recovery of C, N, P and S in the form of algal-bacterial biomass) while minimizing the effluent to be discharged. Process operation in a co-current configuration enabled to maintain this biomass productivity, while counter-current operation decreased biomass productivity likely due to a sulphur-mediated heavy metal deprivation. A bio-methane composition complying with most international regulatory limits for injection into natural gas grids was obtained regardless of the gas/liquid flow configuration. Furthermore, an optimal L/G ratio of 0.5 under co-current flow operation in the AC allowed obtaining a bio-methane composition of 0.8 ± 0.0 % CO_2, 0.01 ± 0.0 % O_2, 0.7 ± 0.2 % N_2 and 98.5 ± 0.2 % CH_4.

We look forward to your evaluation.

Best regards,

Alma Toledo-Cervantes   Raúl Muñoz
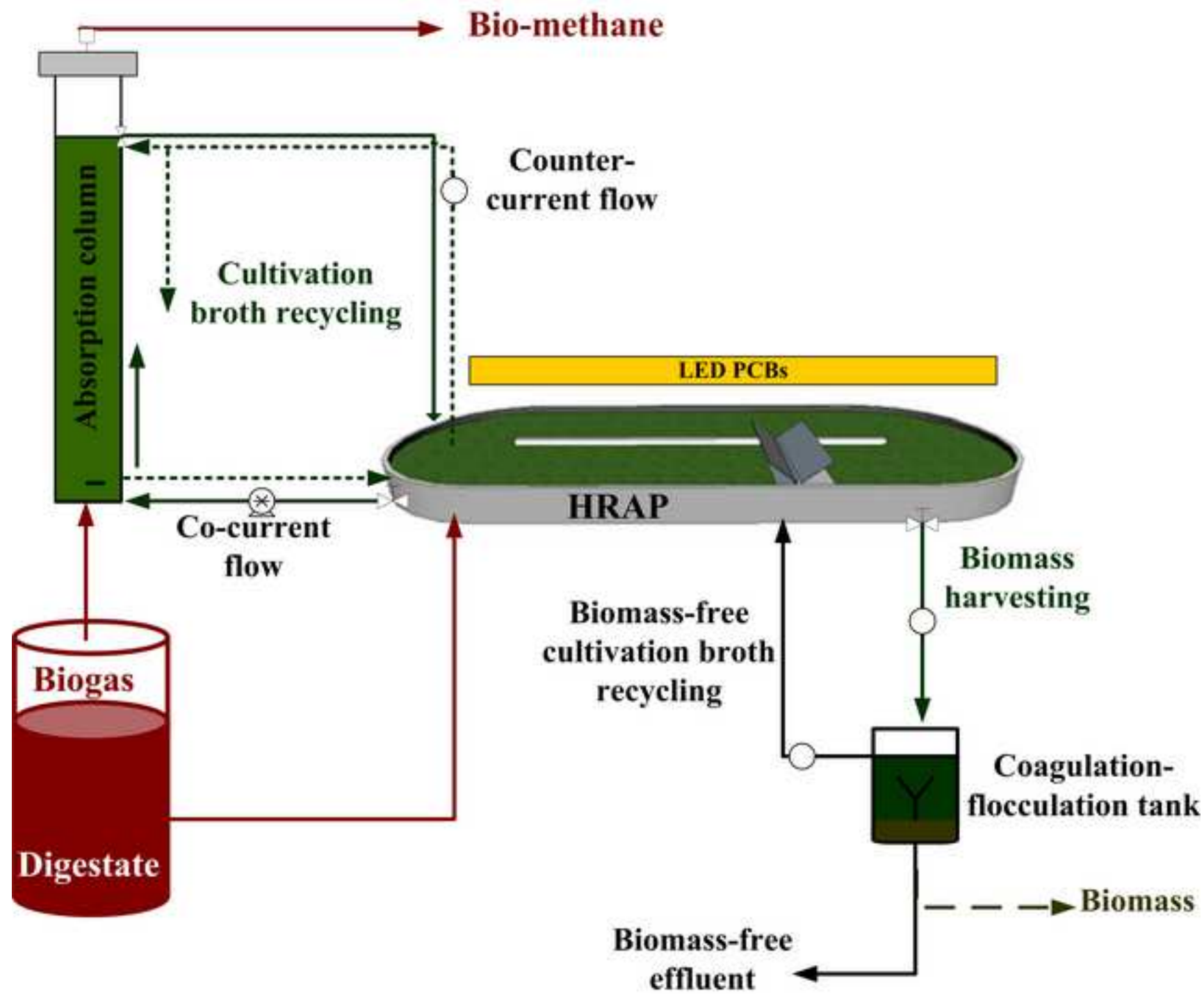
Highlights

- EU standard bio-methane was obtained regardless of the gas-liquid flow configuration

- Optimum bio-methane composition was achieved at a L/G=0.5 under co-current operation

- Counter-current operation decreased biomass productivity and the cultivation broth pH

- High C, N, P and S recoveries were achieved by decoupling the HRT from the SRT

1　　**Influence of the gas-liquid flow configuration in the absorption column on**

2　　**photosynthetic biogas upgrading in algal-bacterial photobioreactors**

3　　Alma Toledo-Cervantes[1], Cindy Madrid-Chirinos[1], Sara Cantera[1], Raquel Lebrero[1],

4　　Raúl Muñoz[1]*

5

6　　1.-Department of Chemical Engineering and Environmental Technology, University of

7　　Valladolid, Dr. Mergelina s/n., Valladolid 47011, Spain.

8

9　　*Corresponding author: mutora@iq.uva.es

10

1

11 **Abstract**

12 The potential of an algal-bacterial system consisting of a high rate algal pond (HRAP)

13 interconnected to an absorption column (AC) via recirculation of the cultivation broth

14 for the upgrading of biogas and digestate was investigated. The influence of the gas-

15 liquid flow configuration in the AC on the photosynthetic biogas upgrading process was

16 assessed. AC operation in a co-current configuration enabled to maintain a biomass

17 productivity of 15 g m^{-2} d^{-1}, while during counter-current operation biomass

18 productivity decreased to 8.7 ± 0.5 g m^{-2} d^{-1} as a result of trace metal limitation. A bio-

19 methane composition complying with most international regulatory limits for injection

20 into natural gas grids was obtained regardless of the gas-liquid flow configuration.

21 Furthermore, the influence of the recycling liquid to biogas flowrate (L/G) ratio on bio-

22 methane quality was assessed under both operational configurations obtaining the best

23 composition at an L/G ratio of 0.5 and co-current flow operation.

24

25 **Keywords:** Algal-bacterial photobioreactor; biogas upgrading; bio-methane; nutrients

26 recovery; digestate.

27

1. Introduction

Anaerobic digestion is a sustainable platform technology to reduce the environmental impact of biodegradable organic wastes. During anaerobic digestion, ~20-95 % of this residual organic matter is biologically converted into biogas (consisting of 50-70 % of CH_4, 30-50 % of CO_2 and trace gases such as H_2S, H_2 and N_2 (Appels *et al*., 2011)) and digestate (a nutrient rich liquid effluent) (Möller and Müller, 2012). Biogas is a renewable energy source typically used in industry for heat and power generation or as natural gas substitute after upgrading. Nowadays, the high energy and chemicals consumption associated to conventional physical-chemical technologies for biogas upgrading (to a CH_4 content of at least 95% as required by most international bio-methane standards) limits their environmental and economic sustainability (Muñoz *et al*., 2015). On the other hand, digestate is applied in agriculture as biofertilizer, although environmental problems such as ammonia emission, nitrate leaching or phosphorus soil saturation might derive from inappropriate digestate handling, storage and application (Holm-Nielsen *et al*., 2009).

In this context, photosynthetic biogas upgrading coupled to nutrient removal from digestate can enhance the sustainability and economic viability of biogas and digestate management (Bahr *et al*., 2014; Posadas *et al*., 2015; Serejo *et al*., 2015). During photosynthetic biogas upgrading, microalgae use light energy to fix the CO_2 from biogas via photosynthesis, while sulphur-oxidizing bacteria oxidize H_2S to sulphate using the O_2 photosynthetically produced. Both microalgal and bacterial growth can be supported by the N and P contained in the digestate, with the subsequent reduction of its eutrophication potential. The algal–bacterial biomass produced during photosynthetic biogas upgrading can be used as slow-release bio-fertilizer or as a feedstock for biofuel

3

53 production, thus contributing to improve the economic and environmental viability of

54 this innovative technology (Posadas *et al*., 2014).

55 Despite the high potential of photosynthetic biogas upgrading, N_2 and O_2 stripping from

56 the recycling cultivation broth to the upgraded biogas often results in CH_4

57 concentrations < 95 %. (Muñoz *et al*., 2015). N_2 and O_2 are often present in the

58 recycling cultivation broth at concentrations of ~14 mg-N_2 L^{-1} and > 8 mg-O_2 L^{-1} as a

59 result of its direct contact with the atmosphere (in open HRAPs) and the intensive

60 microalgal photosynthetic activity in the photobioreactor, respectively (Toledo-

61 Cervantes *et al*., 2016). In fact, the O_2 stripped out from the cultivation broth is a

62 function of the biomass productivity, which is directly linked to the irradiation

63 impinging into the cultivation broth. All studies evaluating the performance of this

64 technology to date were conducted under low light intensities (75-420 μmol m^{-2} s^{-1}),

65 which could have partially biased the results obtained in terms of final bio-methane

66 quality (Posadas *et al*., 2015; Serejo *et al*., 2015; Toledo-Cervantes *et al*., 2016). On the

67 other hand, the liquid to biogas flow (L/G) ratio in the external absorption column (AC)

68 has been recently identified as one of the key operational parameters determining the

69 final composition of bio-methane. Unfortunately, the influence of the biogas/recycling

70 liquid flow configuration in the AC (counter-current *vs* co-current) on bio-methane

71 composition has not been yet systematically assessed. Meier *et al*. (2015) operated a

72 counter-current flow bubble column interconnected to a stirred tank photobioreactor and

73 reported a bio-methane O_2 content of ~1.2 % at a L/G of 6.3. Likewise, bio-methane O_2

74 concentrations ranging from 0.7 to 1.2 were recorded by Posadas *et al*. (2015) in a

75 HRAP interconnected to a bubble column operated at co-current flow. These O_2

76 concentrations were significantly higher than the limit of 0.3 % required by most

77 international regulations for bio-methane injection into natural gas networks, which

78 entails the need for a systematic optimization of biogas scrubbing in the absorption

79 column of photosynthetic biogas upgrading systems.

80

81 This research assessed the influence of the gas-liquid flow configuration (co-current and

82 counter-current) in the AC on bio-methane quality and nutrient recovery performance

83 from real digestate. Additionally, the influence of the L/G ratio (0.3-1) on bio-methane

84 quality was investigated under steady state at the two target gas-liquid flow

85 configurations in order to minimize both O_2 and N_2 content.

86

87 **2. Materials and methods**

88 **2.1 Experimental set-up operation**

89 The experimental set-up consisted of a HRAP interconnected to a bubble column

90 (referred to as absorption column, AC) and to a harvesting tank via recirculation of the

91 cultivation broth (Figure S1, Supplementary information). The system was operated

92 indoors at the Dept. of Chemical Engineering and Environmental Technology at

93 University of Valladolid (Spain). The HRAP dimensions were 170 cm length and 82 cm

94 width, with a working volume of 180 L and an illuminated area of 1.21 m^2. The HRAP

95 was continuously agitated at an internal liquid recirculation velocity of 20 cm s^{-1} and

96 illuminated at 1500 ± 600 µmol m^{-2} s^{-1} by six high intensity LED PCBs (Phillips SA,

97 Spain) using 14:10 h light:dark cycles. The composition of the rendering digestate fed

98 continuously at an influent flow rate of 1 L d^{-1} was (mg L^{-1}): ammonium (NH_4^+) $1668 \pm$

99 249, total nitrogen (TN) 1815 ± 109, total phosphorous (TP) as $P-PO_4^{-3}$ 48 ± 2, chemical

100 oxygen demand (COD) 1745 ± 413, inorganic carbon (IC) 1500 ± 168 and sulphate

101 (SO_4^{-2}) 15 ± 2. Tap water was daily supplied to the HRAP to compensate for

102 evaporation losses. The AC (165 cm height and 4.4 cm diameter) was fed with a

5

103   synthetic biogas mixture (70 % of CH_4, 29.5 % of CO_2 and 0.5 % of H_2S, Abello Linde

104   (Barcelona, Spain)) and cultivation broth from the HRAP at a similar flow rate of 1.6

105   $m^3 m^{-2} h^{-1}$ (flow rate referred to the AC cross sectional area). The algal-bacterial

106   cultivation broth exiting the AC was returned to the HRAP. A fraction of the cultivation

107   broth (26 L d^{-1}) was transferred to an external stirred tank for biomass harvesting, thus

108   decoupling biomass productivity from the hydraulic retention time (HRT). A

109   polyacrylamide-based flocculant solution (Chemifloc CV-300, (de Godos *et al.*, 2011))

110   was dosed at 120 mg L^{-1} to recover the algal-bacterial biomass by coagulation-

111   flocculation. The biomass-free cultivation broth was then returned to the HRAP. This

112   harvesting method represents a low cost alternative for algal-bacterial broths with a

113   sludge volume index > 100 mL g^{-1}. The effluent from the system was removed at 0.5 L

114   d^{-1} from the harvesting tank, along with the flocculated biomass in the stirred tank, in

115   order to minimize the effluent discharged into the environment while avoiding the

116   accumulation of potentially toxic compounds present in the digestate.

117

118   **2.2 Influence of the gas-liquid flow configuration on biogas upgrading and**

119   **nutrients recovery**

120   The HRAP was inoculated with *Mychonastes homosphaera* (Skuja) Kalina &

121   Puncochárová (a taxonomic synonym of *Chlorella minutissima* Fott & Nováková) from

122   a previous culture grown in synthetic anaerobically digested stillage (Toledo-Cervantes

123   *et al.*, 2016). The AC was operated under co-current flow for 94 days (stage I) and for

124   110 days (stage II) under a counter-current flow configuration. Samples of 100 mL from

125   the rendering digestate and the cultivation broth were collected twice a week to measure

126   the pH and concentration of IC, TN, NH_4^+, TP, nitrite (NO_2^-), nitrate (NO_3^-), SO_4^{2-} and

127   TSS. The inlet and outlet biogas flow rate and composition (CO_2, H_2S, O_2, N_2, and CH_4)

128 were also recorded twice a week. Temperature and dissolved O_2 concentration (DO)

129 were *in-situ* determined in the HRAP. Algal-bacterial cultivation broth samples were

130 drawn at each steady state to characterize the structure of the population of both

131 microalgae and bacteria, and their elemental composition (C, N, P and S).

132

133 **2.3 Influence of the L/G ratio on bio-methane composition under co-current and**

134 **counter-current operation**

135 Liquid to biogas flow rate ratios ranging from 0.3 to 1.0 were tested under co-current

136 and counter-current operation. The synthetic biogas was constantly sparged into the AC

137 at 40 mL min^{-1}, while the cultivation broth recycling rate was set at 12, 20, 32 and 40

138 mL min^{-1}. The system was allowed to stabilize for at least two times the liquid HRT

139 before the analysis of bio-methane composition.

140

141 **2.4 Analytical methods**

142 The biogas and bio-methane CO_2, H_2S, O_2, N_2 and CH_4 concentrations were analysed

143 by GC-TCD according to Posadas *et al*., (2015). The DO and pH were monitored with

144 an OXI 330i oximeter (WTW, Germany) and a pH meter Eutech Cyberscan pH 510

145 (Eutech instruments, The Netherlands), respectively. Dissolved TOC, IC and TN

146 concentrations were analysed using a Shimadzu TOC-VCSH analyser (Japan) equipped

147 with a TNM-1 chemiluminescence module. NO_2^-, NO_3^-, PO_4^{-3} and SO_4^{-2} concentrations

148 were measured by HPLC-IC according to Serejo *et al*., (2015), while NH_4^+

149 concentration was determined using an ammonia electrode Orion Dual Star (Thermo

150 Scientific, The Netherlands). COD and TSS analyses were carried out according to

151 standard methods for the examination of wastewater (Eaton *et al*., 2005). The

152 photosynthetic active radiation (PAR) at the HRAP surface was measured with a LI-

153 250A light meter (Lincoln, Nebraska, USA). The biomass C and N content was

154 determined using a CHNS analyser (LECO CHNS-932), while P and S content was

155 analysed by an Inductively Coupled Plasma-Optical Emission Spectrometer (ICP-OES,

156 Varian 725-ES) after microwave-acid digestion (Alcántara *et al*., 2015). The structure of

157 the bacterial population was determined by denaturing gradient gel electrophoresis

158 (DGGE) according to Posadas *et al*., (2015), and the sequences were deposited in

159 GenBank Data Library under accession numbers KX146512-KX146523, while the

160 microalgae community was morphologically characterized by microscopical

161 observations (OLYMPUS IX70, USA) after fixation with 5% of lugol acid.

162

163 **3. Results and discussion**

164 **3.1 Influence of the gas-liquid flow configuration on nutrient recovery from**

165 **rendering digestate**

166 An innovative HRAP operational strategy based on decoupling the HRT from the solids

167 (biomass) retention time (SRT) was applied in this study. This strategy allows

168 maximizing nutrient recovery from high-strength wastewaters (*i.e.* digestate) in the form

169 of algal-bacterial biomass while maintaining biomass concentration below light limiting

170 values (Toledo-Cervantes *et al*., 2016). The system was operated for a period of 2 folds

171 the SRT (25 ± 2 d) before reaching steady state. From day 50 to 94 (stage I), the algal-

172 bacterial consortium was able to maintain a biomass productivity of 15 g m^{-2} d^{-1} with a

173 TSS concentration in the cultivation broth of 2.6 ± 0.3 g L^{-1} (Figure 1, table 1). The high

174 irradiance here applied, which mimicked solar irradiance (1500 ± 600 μmol m^{-2} s^{-1}),

175 prevented excessive mutual shading and supported this dense microalgae culture. The

176 latter was also mediated by the high nutrients concentrations of the high-strength

177 wastewater used. The AC interconnected to the HRAP was operated under counter-

178   current flow configuration from day 104 onwards without a significant variation in the

179   TSS concentration of the HRAP for 7 weeks. However, biomass concentration

180   unexpectedly decreased from day 154 to 167 (Figure 1). In this context, an increase in

181   the phosphorous (P) concentration in the cultivation broth to 4 mg-P L^{-1} was conducted

182   in the HRAP by direct K_2HPO_4 salt addition at day 172 in order to elucidate whether a

183   limitation in this nutrient was responsible for the decrease in the TSS concentration

184   recorded. Phosphorous addition to the cultivation broth stabilized the TSS concentration

185   at 1.3 ± 0.1 g L^{-1} but did not induce the expected 800 mg-TSS L^{-1} concentration increase

186   based on the biomass P content (0.005 g-P/g-biomass). An increment of Mg to 20 mg L^{-}

187   ^{1} by day 181 did not entail an increase in the TSS concentration, which confirmed the

188   absence of magnesium limitation in the cultivation broth. Finally, 180 mL of a

189   micronutrients solution composed of (g L^{-1}) 2.86 H_3BO_3, 1.81 $MnCl_2.4H_2O$, 0.22

190    $ZnSO_4.7H_2O$, 0.39 $Na_2MoO_4.2H_2O$, 0.08 $CuSO_4.5H_2O$, 0.05 $Co(NO_3)_2.6H_2O$ was

191   added at day 195, which led to a rapid increase in TSS concentration up to 2.1 g L^{-1} by

192   day 200. Since no variation in digestate composition occurred over the experimental

193   period, the results herein obtained suggested that microalgae growth was limited by

194   trace metal availability due to their precipitation as sulphur-salts. This sulphur-induced

195   precipitation likely occurred as a result of the O_2 deprivation at the bottom of the AC

196   under counter-current operation, since O_2 was gradually consumed or stripped out on its

197   way downwards (See section 3.2). On the other hand, the DGGE analysis revealed the

198   presence of *Vampirovibrio chlorellavorus* (Band 5 in figure S2, Supplementary

199   information), a non-photosynthetic cyanobacteria and obligate predator that only grows

200   by consuming species of the green alga *Chlorella* (Coder and Goff, 1986; Soo *et al*.,

201   2015). Thus, the combination of a sulphur-mediated heavy metal limitation and the

202   presence of this *Chlorella* predator might have contributed to the decrease in TSS down

203 to 1.4 ± 0.3 g L^{-1}, which only supported a biomass productivity of 8.7 ± 0.5 g m^{-2} d^{-1}.

204

205 The high buffer capacity of the rendering digestate, together with the photosynthetic

206 activity of microalgae mediated by the high productivity imposed during stage I,

207 maintained the pH at 10.2 ± 0.5 and the DO concentration at 15.9 ± 1.6 mg L^{-1}. During

208 stage II, a decrease in the pH and DO concentration of the cultivation broth to 9.5 ± 0.1

209 and 13.3 ± 1.1 mg L^{-1}, respectively, was recorded due to the lower biomass productivity

210 induced by the trace metal limitation (Table 1). These high DO concentrations

211 prevented oxygen limitation during the bacterial oxidation of the organic matter

212 contained in the digestate, and supported COD removal efficiencies (RE) of 83 ± 4.3 %

213 and 89 ± 2.5 % in stages I and II, respectively.

214 Assimilatory rather than abiotic mechanisms governed C, N and P removal during the

215 experiment. A complete removal of NH_4^+ concomitant with a TN-RE of 98 ± 0.4 %

216 were observed in stage I (Figure 2a). Nitrogen assimilation into algal-bacterial biomass

217 during stage I accounted for 64 ± 7 % (0.065 g-N/g-Biomass), $\sim$33% of the N input

218 being stripped out as NH_3 as a result of the high pH of the cultivation broth (10.2). The

219 low nitrification activity observed (Figure 2b) allowed a significant $N-NH_4^+$ removal by

220 stripping. This nitrogen loss would be eventually overcome by either decreasing the N-

221 load or increasing the biomass withdrawal rate from the harvesting tank (a parameter

222 that can be controlled in the experimental set-up) since the digestate nitrogen load

223 selected could theoretically support biomass productivities up to 23 g m^{-2} d^{-1} provided

224 that no other nutrient limitation occurs. In spite of the slight increase in nitrification

225 activity recorded during stage II, the decrease in biomass productivity mediated by

226 counter-current operation resulted in a nitrogen assimilation of 45 ± 12 %, with 49 ± 2

227 % of the N input being stripped out to the environment. Despite the decrease in biomass

228 productivity, P concentration in the cultivation broth remained below the detection limit

229 of the spectrophotometric method used at both operational configurations. The low

230 phosphorous content measured in the biomass (0.005 g-P/g-biomass) and the ability of

231 microalgae to accumulate energy in the form of polyphosphate suggested a total P

232 recovery during both steady states (Alcántara *et al*., 2015).

233 The carbon mass balance conducted estimated that 88 ± 4 % of the carbon supplied

234 (considering both the inorganic and organic carbon in the digestate and the $C\text{-}CO_2$

235 absorbed in the AC) was recovered as biomass during stage I. Carbon recovery

236 decreased in stage II down to 57 ± 5 % due to the above mentioned decrease in biomass

237 productivity. In contrast, IC-RE significantly increased (t-test, $p \leq 0.05$) (Figure 2a) from

238 90 ± 1.1 % to 95 ± 0.5 % mainly due to the enhanced CO_2-stripping (38.6 ± 5 %)

239 mediated by the decrease in pH (Table 1). Additionally, the sulphur mass balance

240 estimated that 38 and 24 % of the sulphur contained in the biogas was assimilated into

241 biomass during stage I and II, respectively (0.007 g-S/g-biomass).

242

243 On the other hand, the alkaline conditions prevailing during HRAP-operation (pH >9.5),

244 together with the high average IC (1550 ± 471 mg L^{-1}) and sulphate (539 ± 113 mg L^{-1})

245 concentrations, promoted the dominance of the unialgal culture of *Mychonastes*

246 *homosphaera* (Skuja) Kalina & Puncochárová. The morphological identification of this

247 microalga was confirmed by the DGGE analysis with observation of bands 2 and 3

248 (Figure S2, Supplementary information), which belonged to the genus *Chlorophyta* and

249 were related to *Chlorella* species. The DGGE analysis also revealed 12 bands belonging

250 to four different phyla: Cyanobacteria/Chloroplast (4 bands), Proteobacteria (5 bands),

251 Chloroflexi (2 bands) and Bacteroidetes (1 band) (Table S1, Supplementary material).

252 Aerobic bacteria from the genus *Sphingomonas* (band 11) and Sphingobacteriales order

253 (band 12) likely supported the biodegradation of the organic matter contained in the

254 digestate (Shokrollahzadeh *et al*., 2008; Ye and Zhang, 2013)

255

256 Finally, the low effluent flow rate (0.5 L d^{-1}), together with the low N and P effluent

257 concentrations recorded, entailed a low environmental impact in terms of wastewater

258 discharge to the environment. At this point it should be also stressed that the

259 coagulation-flocculation process implemented in the interconnected tank was efficient

260 at removing biomass from the cultivation broth to an average effluent TSS

261 concentration of 28 ± 4 mg L^{-1}, which complies with the limit established by the

262 European Union legislation (European Directive 91/271/CEE).

263

264 **3.2 Influence of gas-liquid flow configuration on biogas upgrading performance**

265 Conventional water scrubbing for biogas upgrading relies on the contact between the

266 biogas flowing upwards through a packed absorption column and a pressurized water

267 stream trickling down in a counter-current mode. The column is typically filled with

268 random packing materials in order to increase the specific gas-liquid contact area and

269 thus maximize the gas-liquid mass transfer. State of the art water scrubbers can provide

270 a bio-methane with a CH_4 content of 96-98 % (Ryckebosch *et al*., 2011). In contrast, the

271 absorption columns coupled to photobioreactors have been mostly operated at co-

272 current flow with no packing materials to avoid biomass clogging (Toledo-Cervantes *et*

273 *al*., 2016), with only one experimental study conducted using a counter-current flow

274 configuration (Meier *et al*., 2015). The study here reported constitutes, to the best of our

275 knowledge, the first systematic comparison addressing the influence of the biogas-

276 recycling liquid flow configuration on bio-methane composition. Statistically different

277 (t-test, p$\leq$ 0.05) CO_2-REs of 98.8 ± 0.8 % (co-current) and 96.9 ± 1.6 % (counter-

278   current) were recorded during stages I and II, respectively, while statistically similar

279   REs ~100 % were obtained for H_2S. The CO_2 and H_2S REs observed under a co-current

280   configuration were in agreement with those reported by Toledo-Cervantes *et al*. (2016).

281   The lower CO_2-REs recorded under counter-current flow operation were attributed to

282   the decrease in the pH of the cultivation broth from 10.2 to 9.5 (Table 1), mediated by

283   the decrease in microalgal photosynthetic activity (See section 3.1). These results

284   confirmed that CO_2 removal highly depends on the photosynthetic activity of

285   microalgae in spite of the high buffer capacity of the digestate. Furthermore, the nearly

286   complete H_2S removal observed at both configurations highlighted the robustness of

287   this biological technology for the abatement of H_2S from biogas.

288

289   Table 2 shows the bio-methane composition under co-current and counter-current flow

290   configurations. The CO_2 and CH_4 contents of the bio-methane were statistically

291   different, with a higher CH_4 content under a co-current flow configuration (96.2 $\pm$ 0.7

292   %) (Figure 3a). The bio-methane obtained in both operational stages presented a low

293   oxygen content due to the active oxygen demand resulting from the oxidation of H_2S to

294   sulphate (Figure 3b). No significant differences in O_2 and N_2 content were observed at

295   both operational configurations. Toledo-Cervantes *et al*. (2016) reported a similar N_2

296   concentration (2.4 $\pm$ 0.2 %) but a lower O_2 content (0.03 $\pm$ 0.04 %) in the biogas

297   upgraded in a similar experimental set-up operated under co-current flow configuration

298   at a L/G=1. The lower O_2 content observed by these authors was likely due to the lower

299   irradiance (420 $\pm$ 105 μmolm^{-2} s^{-1}) and biomass productivity (7.5 g m^{-2} L^{-1}) used in

300   their experimentation, which entailed a lower DO concentration in the cultivation broth

301   (9.6 $\pm$ 0.4 mg O_2 L^{-1}). Moreover, since the same L/G ratio was applied at both

302   operational configurations, the nitrogen content in the bio-methane (stripped out from

303   the cultivation broth) was statistically similar (Figure 3b).

304

305   The bio-methane obtained under both gas-liquid flow configurations complied with the

306   regulatory limits of most international standards for bio-methane injection into natural

307   gas grids regardless of the operational configuration. Nonetheless, several operational

308   problems were observed during counter-current flow operation. First, elemental sulphur

309   accumulation at the bottom of the AC resulted in diffuser clogging, while biomass

310   accumulation at the top of the AC caused the obstruction of pipelines. The elemental

311   sulphur accumulation observed under counter-current configuration was attributed to

312   the stripping and gradual DO consumption along the AC, which resulted in a low DO

313   concentration at the bottom of the AC where biogas was sparged. Therefore, the

314   dissolved H_2S at the bottom of the column was not completely oxidized to sulphate but

315   to elemental sulphur, which accumulated at the surface of the diffuser and the

316   absorption column's walls. The limited H_2S oxidation at the bottom of the AC was also

317   responsible of the trace metal precipitation hypothesized in section 3.1.

318

319   **3.3 Influence of the L/G ratio on bio-methane composition under co-current and**

320   **counter-current operation**

321   The recycling liquid to biogas ratio constitutes as a key operational parameter

322   determining the final quality of bio-methane in algal-bacterial photobioreactors

323   (Toledo-Cervantes *et al*., 2016). Theoretically, an increased overall concentration

324   gradient and volumetric mass transfer coefficient were expected under counter-current

325   flow operation. Nonetheless, the decrease in pH and biomass productivity during stage

326   II counterbalanced the beneficial mass transfer effects of counter-current flow

327   operation. In this context, a systematic evaluation of the influence of the L/G ratio on

14

328   bio-methane composition was carried under both gas-liquid flow configuration. This

329   experimentation was carried out from days 95 to 98 and therefore it was not biased by

330   the above-mentioned secondary effects of the counter-current flow operation on the

331   cultivation broth (*i.e.* lower biomass productivity and pH) and allowed to minimize the

332   O_2 and N_2 content in the bio-methane without compromising the CO_2 removal.

333

334   Table 3 shows the REs recorded under both gas-liquid flow configurations. The CO_2-

335   REs at the L/G ratios tested were significantly different under co-current and counter-

336   current flow operation (t-test, $p \leq 0.05$), except for the REs obtained under counter-

337   current flow operation at a L/G ratio of 1 and 0.8. The CO_2-REs observed at a L/G ratio

338   of 1 were in agreement with those previously reported by Toledo-Cervantes *et al*.

339   (2016) (98.8 ± 0.2 %) using a similar experimental fed with synthetic digestate. The

340   results obtained also indicated that the CO_2-REs increased at increasing the L/G ratio up

341   to 1, likely due to the higher carry over capacity when increasing the recycling liquid

342   rate. As expected, higher CO_2-REs were observed under counter-current flow operation

343   (Table 3) due to the enhanced overall concentration gradient and mass transfer

344   coefficient (k_{La}-CO_2), the latter mediated by an extended gas-liquid contact time. In

345   contrast, the CO_2-REs recorded at a L/G ratio of 0.3 were lower at both operational

346   configurations (70.3 ± 1.0 % and 60.4 ± 1.9 % under co-current and counter-current

347   flow operation, respectively). These low CO_2-REs were attributed to the decrease in pH

348   in the recycling cultivation broth from 10 to 8.5 ± 0.1 induced by the increase in the

349   liquid HRT in the AC. No significant differences were observed in the H_2S-REs under

350   both operational configurations regardless of the L/G ratio, which confirmed the

351   robustness of this technology in terms of H_2S.

352

353 Counter-current flow operation involved higher mass transfer rates, which resulted in

354 higher O_2 and N_2 desorption rates from the cultivation broth concomitant with enhanced

355 CO_2 removals in the AC, but slightly lower CH_4 concentrations than under co-current

356 operation (Figure 4). However, the two gas-liquid flow configurations tested allowed

357 obtaining a bio-methane complying with most international regulations. Under co-

358 current flow operation at a L/G of 0.5, a bio-methane composition of 0.8 ± 0.0 % of

359 CO_2, 0.01 ± 0.0 % of O_2, 0.7 ± 0.2 % of N_2 and 98.5 ± 0.2 % of CH_4 was obtained,

360 which to the best of our knowledge constitutes the best composition ever reported for

361 any stand-alone biological biogas upgrading technology.

362

363 **4. Conclusions**

364 Microalgae photosynthetic activity was identified as a key process parameter

365 determining both the quality of bio-methane and the extent of the nutrients removal

366 mechanisms. Process design here evaluated, allowed decoupling biomass productivity

367 from the HRT, which overcame the light limitation problem associated with the use of

368 high strength digestates. Despite counter-current flow operation supported a more

369 efficient gas-liquid mass transfer, both the enhanced N_2/O_2 stripping and the lower

370 microalgal activity observed, resulted in a lower bio-methane quality. However, the bio-

371 methane composition achieved under both operational configurations complied with the

372 regulatory limits required for its injection into natural gas grids.

373

381

382   References

383   [1]   Alcántara, C., Fernández, P.A., García-Encina, R. Muñoz. Mixotrophic

384   metabolism of *Chlorella sorokiniana* and algal-bacterial consortia under extended dark-

385   light periods and nutrient starvation. *Appl. Microbiol. Biotechnol*. 2015, 99 (5), 2393-

386   2404

387   [2]   Appels, L., Lauwers, J., Degrève, J., Helsen, L., Lievens, B., Willems,

388   K., Impe, J.V., Dewil, R. 2011. Anaerobic digestion in global bio-energy production:

389   Potential and research challenges. *Renew. Sust. Energ. Rev.* 2011, 15 (9), 4295-4301

390   [3]   Bahr, M., Díaz, I., Domínguez, A., González Sánchez, A., Muñoz, R.

391   Microalgal-biotechnology as a platform for an integral biogas upgrading and nutrient

392   removal from anaerobic effluents. *Environ. Sci. Technol*. 2014, 48, 573-581

393   [4]   Coder, D.M., Goff, L.J. The host range of the Chlorellavorous bacterium

394   ("*Vampirovibrio chlorellvorus*"). *J. Phycol.* 1986, *22* (4), 543-546

395   [5]   de Godos, I., Guzman, H.O., Soto, R., García-Encina, P.A., Becares, E.,

396   Muñoz, R., Vargas, V.A. Coagulation/flocculation-based removal of algal–bacterial

397   biomass from piggery wastewater treatment, *Bioresour. Technol*. 2011, 102 (2), 923-

398   927

399   [6]   Eaton A.D., Clesceri L.S., Greenberg A.E. Standard methods for the

400   examination of water and wastewater. 21 st edition. 2005. American Public Health

401   Association/American Water Works Association/ Water Environment Federation

402   [7]   European Directive 91/271/CEE on discharge of domestic wastewaters,

403   1991

404   [8]   Holm-Nielsen, J.B., Seadi, T.A., Oleskowicz-Popiel, P. The future of

405   anaerobic digestion and biogas utilization. *Bioresour. Technol*. 2009, 100 (22), 5478-

406   5484

407   [9]   Möller, K., Müller, T. Effects of anaerobic digestion on digestate nutrient

408   availability and crop growth: A review. *Eng. Life Sci.* 2012, 12 (3), 242–257

409   [10]   Muñoz, R., Meier, L., Díaz, I., Jeison, D. A review on the state-of-the-art

410   of physical/chemical and biological technologies for biogas upgrading. *Rev Environ Sci*

411   *Biotechnol*. 2015, 14 (4), 727-759

412   [11]   Posadas, E., Bochon, S., Coca, M., García-González, M.C., García-

413   Encina, P.A., Muñoz, R. Microalgae-based agro-industrial wastewater treatment: a

414   preliminary screening of biodegradability. *J. Appl. Phycol.* 2014, 26, 2335-2345

415   [12]   Posadas, E., Serejo, M., Blanco, S., Pérez, R., García-Encina, P.A.,

416   Muñoz, R. Minimization of bio-methane oxygen concentration during biogas upgrading

417   in algal–bacterial photobioreactors. *Algal Research*. 2015, 12, 221-229

418   [13]   Ryckebosch, E., Drouillon, M. and Vervaeren, H., Techniques for

419   transformation of biogas to biomethane. *Biomass bioenergy*, 2011, *35* (5), 1633-1645

420   [14]   Serejo, M., Posadas, E., Boncz, M., Blanco, S., García-Encina, PA.,

421   Muñoz, R. Influence of biogas flow rate on biomass composition during the

422   optimization of biogas upgrading in microalgal-bacterial processes. *Environ. Sci.*

423   *Technol.* 2015, 49, 3228-3236

424   [15]   Shokrollahzadeh, S., Azizmohseni, F., Golmohammad, F., Shokouhi, H.

425   and Khademhaghighat, F. Biodegradation potential and bacterial diversity of a

426   petrochemical wastewater treatment plant in Iran. *Bioresour. Technol*. 2008, 99(14),

427   6127-6133.

428   [16]   Soo, R.M., Woodcroft, B.J., Parks, D.H., Tyson, G.W. Hugenholtz, P.

429   Back from the dead; the curious tale of the predatory cyanobacterium Vampirovibrio

430   chlorellavorus. *Peer J*. 2015, *3*, e968

431   [17]   Tippayawong, N., Thanompongchart, P. Biogas quality upgrade by

432   simultaneous removal of CO_2 and H_2S in a packed column reactor. *Energy*. 2010, 35

433   (12), 4531-4535

434   [18]   Toledo-Cervantes, A., Serejo, M., Blanco, S., Pérez, R., Lebrero, R.,

435   Muñoz, R. Photosynthetic biogas upgrading to bio-methane: boosting nutrient recovery

436   via biomass productivity control. *Algal Research*. 2016, 17, 46-52

437   [19]   Uggetti, E., Sialve, B., Latrille, E., Steyer, J-P. Anaerobic digestate as

438   substrate for microalgae culture: The role of ammonium concentration on the

439   microalgae productivity, *Bioresour. Technol*. 2014, 152, 437-443

440   [20]   Ye, L. and Zhang, T. Bacterial communities in different sections of a

441   municipal wastewater treatment plant revealed by 16S rDNA 454 pyrosequencing.

442   *Appl. Microbiol. Biot*. 2013, 97(6), 2681-2690.

443   **Figure caption.**

444

445   **Figure 1.** Time course of the total suspended solids concentration in the HRAP. The

446   vertical line indicates the change in the gas-liquid flow configuration in the AC.

447
448   **Figure 2. a)** Removal efficiencies of chemical oxygen demand (COD), ammonium

449   (NH_4^+), total nitrogen (TN), inorganic carbon (IC), sulphate (SO_4^{-2}) and phosphate (PO_4^-

450   ^{3}) in the HRAP and **b)** effluent concentrations of nitrate ($N-NO_3^-$), nitrite ($N-NO_2^-$) and

451   sulfate (SO_4^{-2}) under co-current (black bars) and counter-current (white bars) gas-liquid

452   flow operation. Vertical lines represent standard deviations from replicate

453   measurements under steady state operation. All REs were significantly different (t-

454   student test, p<0.05) except those of NH_4^+ and PO_4^{-3}.

455
456   **Figure 3.** Time course of the concentration of **a)** CO_2 (○) and CH_4 (Δ), and **b)** O_2 (□)

457   and N_2 (◊) in the bio-methane. Vertical lines represent standard deviations from

458   replicate measurements.

459
460   **Figure 4.** Influence of the recycling liquid to biogas ratio on the concentration of **a)** O_2,

461   **b)** N_2, **c)** CH_4 and **d)** CO_2 in the bio-methane under co-current (□) and counter-current

462   (○) gas-liquid flow operation. Vertical lines represent standard deviations from replicate
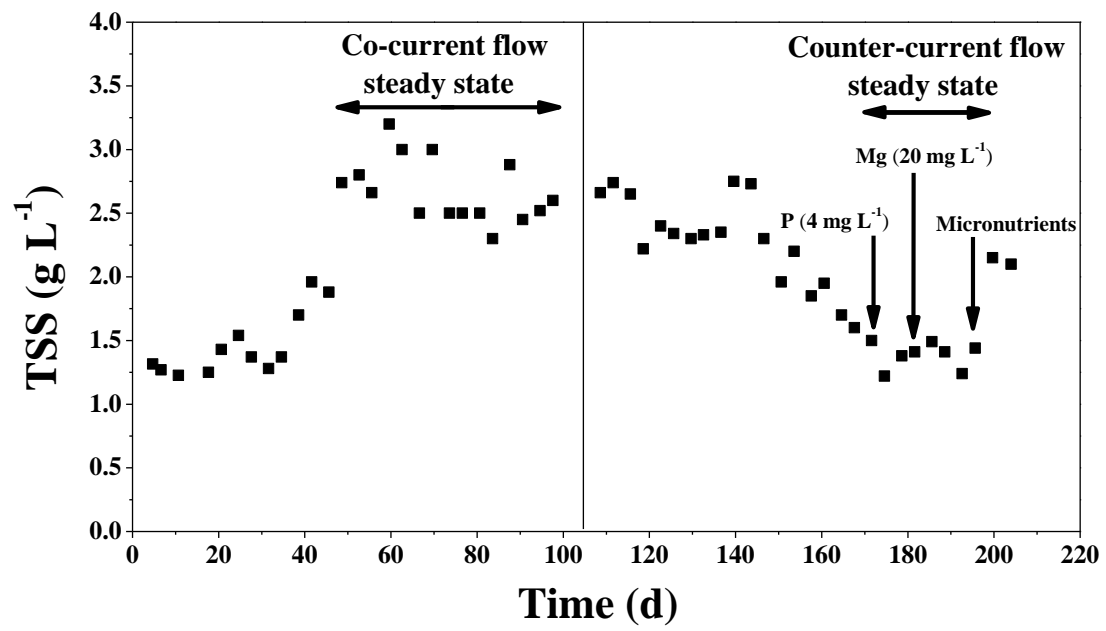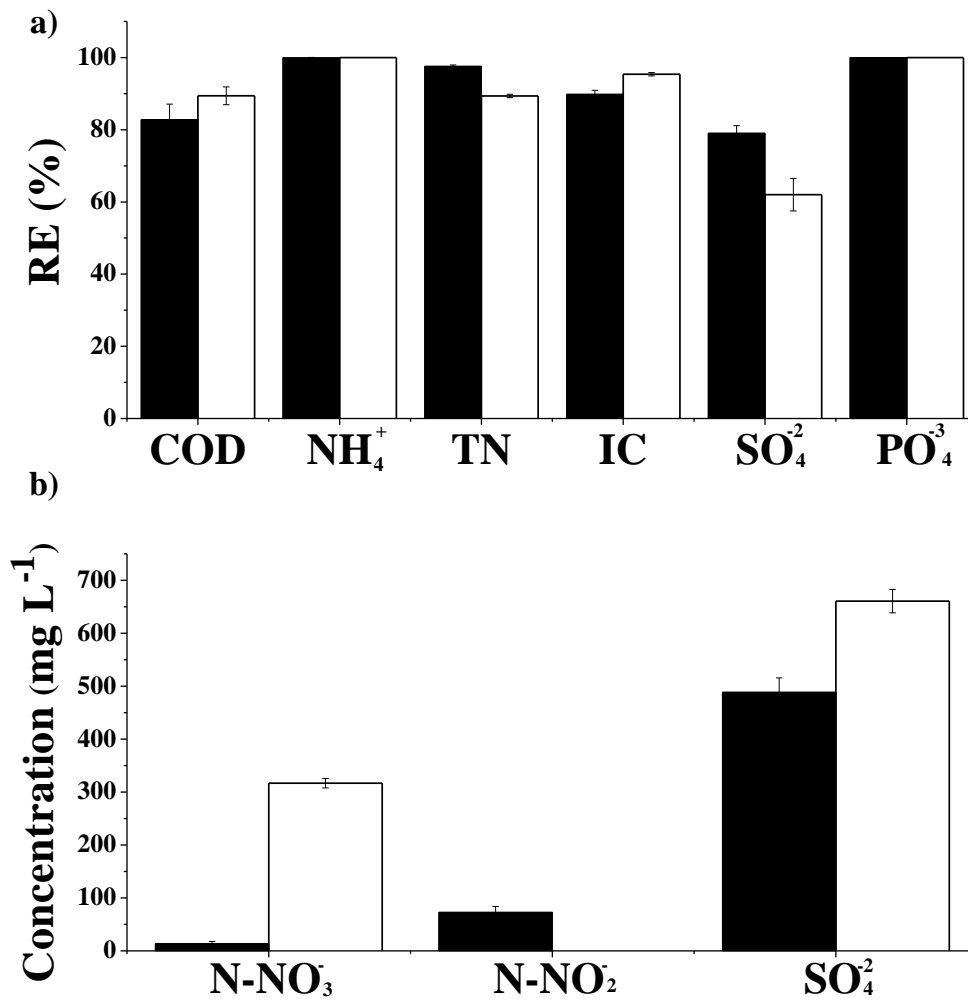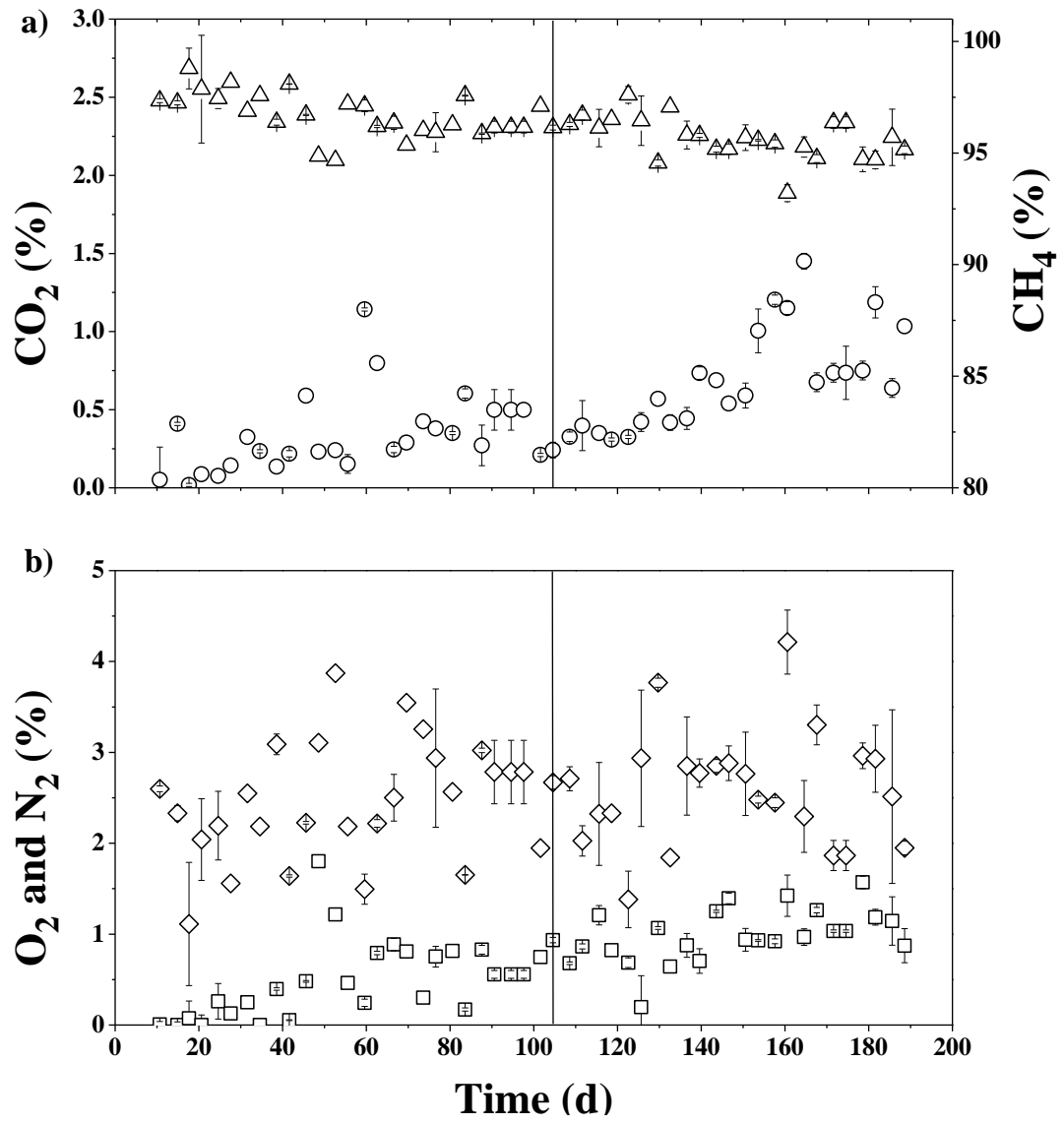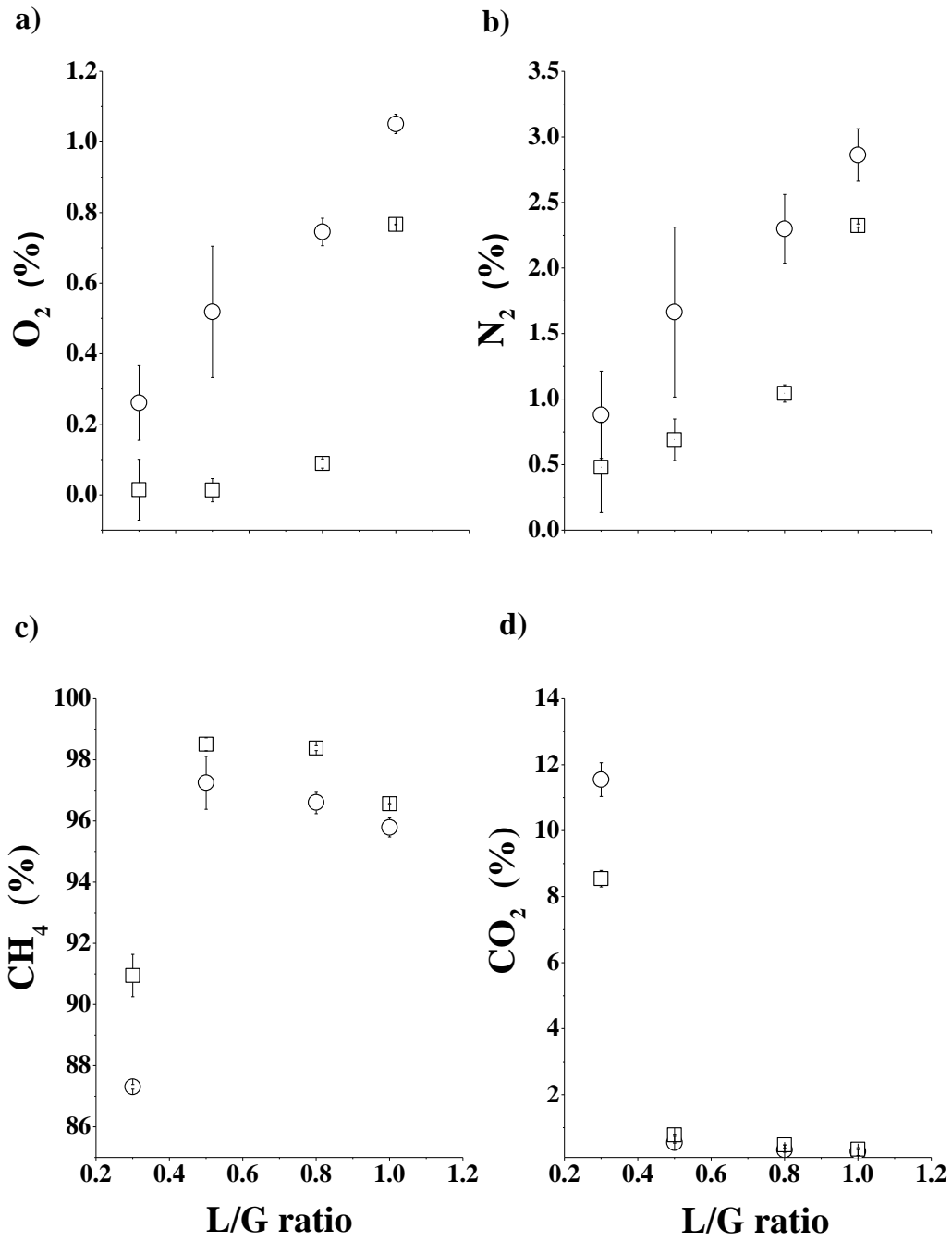
463   measurements.

Figure 1.

Figure 2.

a)

b)

Figure 3.

Figure 4.

a)

b)

c)

d)

Table

	HRAP (°C)	TSS	pH-digestate	pH-HRAP	DO (mg L^{-1})
Co-current flow	23.8 ±1.7	2.6 ± 0.3	7.8 ±0.4	10.2 ±0.5	15.9 ±1.6
Counter-current flow	19.4 ±1.6	1.4 ± 0.3	7.6 ±0.2	9.5 ±0.1	13.3 ±1.1

Table 1. Operating conditions under co-current and counter-current flow configurations in the absorption column.

Table 2. Average steady state bio-methane composition under co-current and counter-current flow configurations in the absorption column.				
	CO_2 (%)	**O_2 (%)**	**N_2 (%)**	**CH_4 (%)**
Co-current flow	0.4 ± 0.3	0.7 ± 0.4 [a]	2.7 ± 0.5 [b]	96.2 ± 0.7
Counter-current flow	0.9 ± 0.3	1.2 ± 0.3 [a]	2.6 ± 0.3 [b]	95.1 ± 0.2
*Same letter means no significantly different (t-test, p$\leq$ 0.05)				

Table 3. Influence of the L/G ratio on the carbon dioxide and hydrogen sulphide removal efficiencies under co-current and counter-current flow configurations in the absorption column.

L/G ratios	RE at co-current flow (%)		RE at counter-current flow (%)	
	CO_2	H_2S	CO_2	H_2S
1	98.8 ± 0.0	100 [a]	99.2 ± 0.1 [b]	99.2 ± 1.4 [a]
0.8	98.3 ± 0.0	100 [a]	98.9 ± 0.2 [b]	96.1 ± 3.6 [a]
0.5	97.3 ± 0.1	100 [a]	98.1 ± 0.1	98.3 ± 1.4 [a]
0.3	70.3 ± 1.0	98.3 ± 2.4 [a]	60.4 ± 1.9	100 [a]
*Same letter means no significantly different (t-test, $P \leq 0.05$)				

Electronic Annex

Click here to download Electronic Annex: Supplementary information.docx